Comp. & Maths. with Appls., Vol. 3, pp. 53–63. Pergamon Press 1977. Printed in Great Britain

DOWNSTREAM BOUNDARY CONDITIONS FOR VISCOUS FLOW PROBLEMS

GEORGE FIX

Department of Mathematics, Carnegie–Mellon University, Pittsburgh, PA 15213, U.S.A.

and

MAX GUNZBURGER

Institute for Computer Applications in Science and Engineering, Hampton, VA 23665, U.S.A.

Communicated by E. Y. Rodin

(*Received September*, 1976)

Abstract—The problem of the specification of artifical outflow conditions in flow problems is studied. It is shown that for transport type equations incorrect outflow conditions will adversely affect the solution only in a small region near the outflow boundary, while for elliptic equations, e.g. those governing the streamfunction or pressure, a correct boundary specification is essential. In addition, integral outflow boundary conditions for fluid dynamical problems are considered. It is shown that such conditions are well posed, and their effect on the solutions of the Navier–Stokes equations is also considered.

I. INTRODUCTION

The selection of appropriate boundary conditions to use on outflow regions has been a classical problem in computational fluid dynamics. Normally, the outflow boundaries are artificial in the sense that they are arbitrarily supplied so that the physical problem can be defined in a bounded region. A typical situation is given in Fig. 1, and represents a flow in an expanding channel. The inflow conditions in effect define the problem. Thus along AG in Fig. 1 we specify u and v which are the x and y components of the velocity field. Along a solid wall such as AC the correct boundary conditions are that there is no flow through the wall, i.e. $v = 0$, and with viscous forces present, that there is no flow tangent to the wall, i.e. $u = 0$. The problem arises at the outflow CD. This line was added in order to make the computational domain Ω finite, and since it occurs in the fluid itself, correct boundary conditions along this line are by no means clear either mathematically or physically.

It is not surprising that the literature of the downstream boundary condition problem is apparently contradictory. For example, Chen [1], reported numerical experiments that indicated that for transport type equations, almost anything could be specified provided that the outflow boundary (such as BC in Fig. 1) was far enough downstream, i.e. away from corner points such as E. On the other hand Roache [2] specifically suggests the use of downstream continuation which in effect sets second derivatives equal to zero on the outflow BC.

In particular applications, e.g. Paris and Whitaker [3] and Cerro and Whitaker [4], authors also used function values or first derivative values for downstream boundary conditions. It is usually the case that in such successful computations the downstream boundary is placed so far downstream that the prescribed boundary conditions are indeed accurate. In addition, various authors, e.g. Cerro and Whitaker [5] and Ghia [6], map the infinite domain into a finite one. They then impose true (or at least asymptotically correct) infinity conditions. Although this approach is useful for many problems, we do not consider it in the present work because we are interested in determining the effects of imposing incorrect outflow conditions and in many areas, such as limited region ocean circulation problems, mapping techniques are not applicable.

In this paper we show that if the problem is formulated in terms of the streamfunction ψ and the vorticity ζ

$$\frac{\partial \zeta}{\partial t} + \frac{\partial \psi}{\partial y}\frac{\partial \zeta}{\partial x} - \frac{\partial \psi}{\partial x}\frac{\partial \zeta}{\partial y} = \frac{1}{R}\Delta\zeta \tag{1.1}$$

$$\nabla^2 \psi = \zeta \tag{1.2}$$

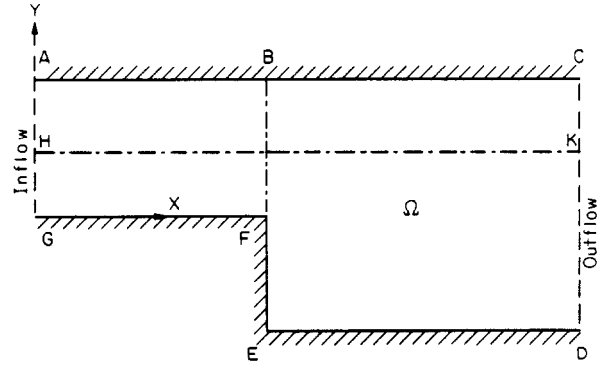

Fig. 1. Flow in a channel.

then any specification of vorticity on the outflow yields sufficiently accurate solutions of (1.1) independent of the downstream positions of the outflow boundary. Indeed, a change in the outflow specification of the vorticity will affect the solution only in a small boundary layer near the outflow. This is verified in Section 2 for one dimensional problems and in Section 3 for two dimension problems. In addition, it is verified for a representative difference scheme.

On the other hand the situation is entirely different for the elliptic equation (1.2). Differences in outflow specification significantly propagate into the interior and therefore it is crucial that the correct outflow condition on the streamfunction be specified. Thus as the outflow is moved far downstream it is known that indeed $\partial^2\psi/\partial x^2$ approaches zero on the outflow, or alternately, since one knows the flow at large distances from E, one could just as well specify ψ or $\partial\psi/\partial x$ along CD. However, if the outflow is moved in or if one is dealing with problems where there are no known asymptotic downstream solutions, specification of these quantities will yield spurious solutions.

In many problems of the latter type integral conditions on the flow can be accurately estimated. For example, in limited region ocean circulation problems, mass flows, i.e. volume integrals of the flow, can be measured [7]. Furthermore, in many situations, integrals conditions on the flow can be accurately specified in the steady state. In this paper we consider, apparently for the first time, integral boundary conditions for (1.1) and (1.2). Conditions of this type are included in the work presented in Sections 2 and 3. Moreover, in Section 4 we indicate that such problems are well posed and that a representative finite difference scheme is not adversely affected by the integral boundary conditions.

2 A SIMPLE 1-D EXAMPLE FOR THE TRANSPORT EQUATION

We wish to study the effects due to the specification of outflow conditions on a transport equation such as (1.1). To illustrate the main ideas we begin with the linear equation

$$\frac{\partial w}{\partial t}+\frac{\partial w}{\partial x}=\frac{1}{R}\frac{\partial^2 w}{\partial x^2}, \qquad 0<x<1. \tag{2.1}$$

At the inflow, $x=0$, we specify

$$w(0,t)=w_{\text{in}}(t). \tag{2.2}$$

Three alternatives will be considered for outflow boundary conditions, two of which are in common use. The first condition, hereafter Option A, is to specify

$$w(1,t)=w_{\text{out}}(t). \tag{2.3}$$

The second, commonly called downstream continuation and in this paper denoted as Option B, is

$$\partial^2 w/\partial x^2(1,t)=0. \tag{2.4}$$

Option C is the integral condition

$$\int_0^1 w(x,t)\,dx = m(t). \tag{2.5}$$

Other outflow conditions, such as specifying the first derivative, could also be considered. Their effects could be deduced in a similar manner to the following development for Options *A*, *B* and *C*.

The disadvantages of Options *A* and *C* are that one does not usually know w_{out} and m although in some situations, especially steady state ones, m can be accurately estimated. The disadvantage of Option *B* is that it may not be consistent with the type of flow that is being modeled. There is also the mathematical problem involved with the specification of higher order derivatives on the boundary. We assert, nevertheless, that in each case the errors in the solution of (2.1) are restricted to an outflow boundary layer.

Before proving these assertions, let us consider discrete analogs for (2.1)–(2.5). To keep the analysis simple, we choose the simple explicit finite difference approximation to (2.1)

$$(w_j^{n+1} - w_j^n)/\tau + (w_{j+1}^n - w_{j-1}^n)/2h = (w_{j+1}^n - 2w_j^n + w_{j-1}^n)/Rh^2 \tag{2.6}$$

for $1 < j \le J-1$ and $n \ge 0$, where $J = 1/h$, h and τ are the uniform grid sizes in x and t, respectively, and $w_j^n \approx w(jh, n\tau)$. The three boundary conditions in addition to the inflow condition

$$w_0^n = w_{in}(n\tau) \tag{2.7}$$

are

$$A: \quad w_J^n = w_{out}(n\tau) \tag{2.8}$$

$$B: \quad w_J^n - 2w_{J-1}^n + w_{J-2}^n = 0 \tag{2.9}$$

and

$$C: \quad h\sum_{j=0}^{J-1} [w_j^n + w_{j+1}^n] = 2m(n\tau) \tag{2.10}$$

The last equation is obtained from (2.5) *via* trapezoidal quadratures.

Before analysing (2.1)–(2.5) and (2.6)–(2.10), we report some numerical experiments. First we consider the problem whose exact solution is known, namely

$$W(x,t) = \sin(ax - at)\exp(-a^2 t/R).$$

Then, for our computations we take the inflow and initial conditions to be $W(0, n\tau)$ and $W(jh, 0)$, respectively. We arbitrarily specify $w_{out} = m = 0$ so that all three outflow conditions are in error. Figures 2 and 3 show the pointwise error resulting from the computations, i.e.

$$E_j^n = w_j^n - W(jh, n\tau)$$

as a function of x for different values of t. The parameters used are $J = 50$, $\tau = 0.001$, $a = 4.5\pi$, $R = 10$ for Fig. 2 and $R = 20$ for Fig. 3. The initial condition on W is also shown in order to provide a reference scale. Note that for all three options, $E_j^n \approx 0$ for a large part of the domain $0 \le x \le 1$ and that E_j^n in large only near the outflow boundary. The thickness of the region in which errors occur is essentially the same for all three options. Furthermore, for $R = 20$, the thickness of the boundary layer is smaller than for $R = 10$. This is especially evident for Option *C*, where the boundary layer is quite pronounced. In fact, from tabular data, it can be shown for all three options that the boundary layer thickness δ obeys the empirical relation

$$\delta \sim 1/R \tag{2.11}$$

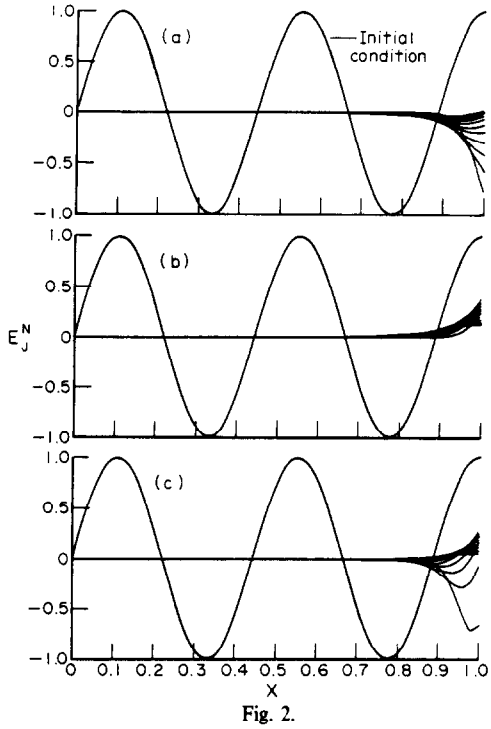

Fig. 2.

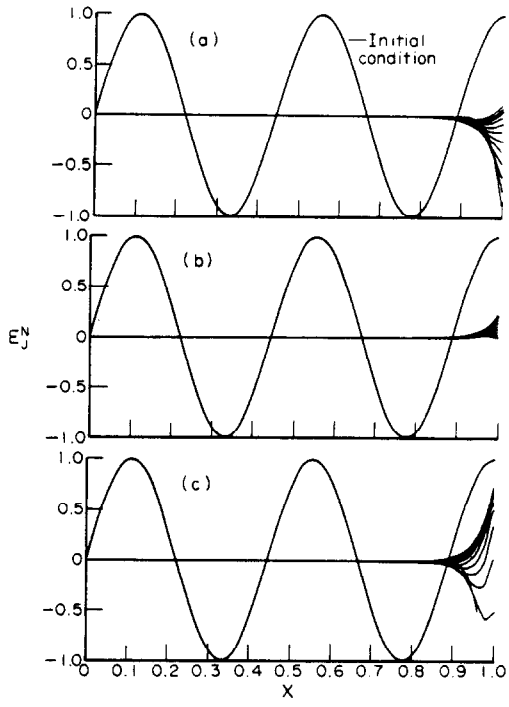

Fig. 3.

Fig. 2. E_j^n vs x for $R = 10, J = 50, \Delta t = 0.001$. Plotted every $12\Delta t$.

Fig. 3. E_j^n vs x for $R = 20, J = 50, \Delta t = 0.001$. Plotted every $12\Delta t$.

where $\delta = 1 - x_B$ and x_B is the smallest value of x at which the error is a given small percentage of the maximum error along a particular curve. The relation (2.11) is largely independent of the choice of the "given small percentage."

We next turn to an example, again for (2.1), whose transient solution is not known, but for which the graph of the solution is simple enough so that the transient can be easily followed. We consider

$$w(x,0) = b \exp\{-(x-c)^2/d^2\} \quad \text{and} \quad w(0,t) = 0$$

to be the initial and inflow conditions, respectively. Then the steady state solution of (2.1) in the semi-infinite domain $0 \le x \le \infty$ is zero. We take as outflow conditions

$$w_{\text{out}} = A \quad \partial^2 w/\partial x^2|_{x=1} = B \quad \text{and} \quad m = C \tag{2.12}$$

so that all three outflow conditions are in error, even in the steady state. A, B and C are interpretated as being errors in the specification of the corresponding outflow condition. Figure 4 shows w as a function of x for different values of t with $J = 50$, $\tau = 0.0025$, $b = 10$, $c = 0.8$, $d = 0.05$ and $A = B = C = 1$. The steady state solution fails to vanish only in a region near the outflow boundary regardless of the option chosen so that again errors due to the incorrect specification of outflow conditions are trapped in a boundary layer near the outflow. Experiments at different Reynolds' numbers confirm the reciprocal relation (2.11). For Fig. 5, the computations of Fig. 4 are repeated for $A = B = C = 0$, so that the outflow conditions are correct for the steady state but not for the transient solution. The correct steady state is now achieved for all x for all three options. Furthermore, comparing Figs. 4 and 5, we see that except for a small region near the outflow, all six transient solutions are in good agreement. This indicates that away from the outflow boundary, the transient solution is correctly computed not only regardless of which option is chosen, but independent of the actual numerical values of A, B and C chosen in (2.12).

Many other experiments were performed, both on (2.1) and on nonlinear equations such as Burgers' equation. In all cases the boundary layer phenomena reported above was reproduced, and

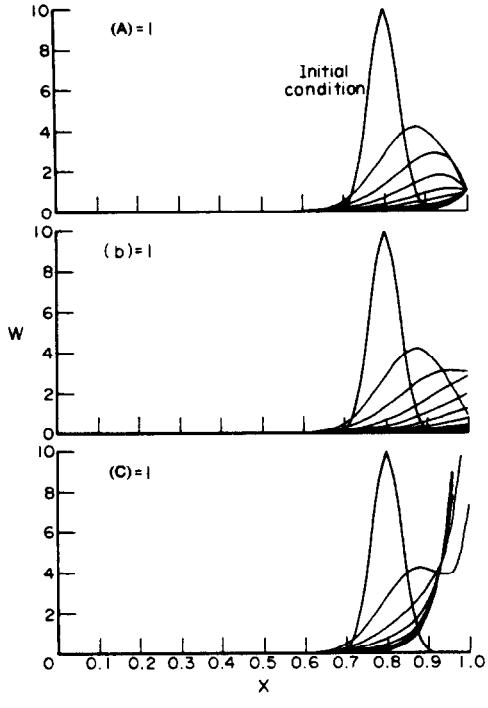

Fig. 4.

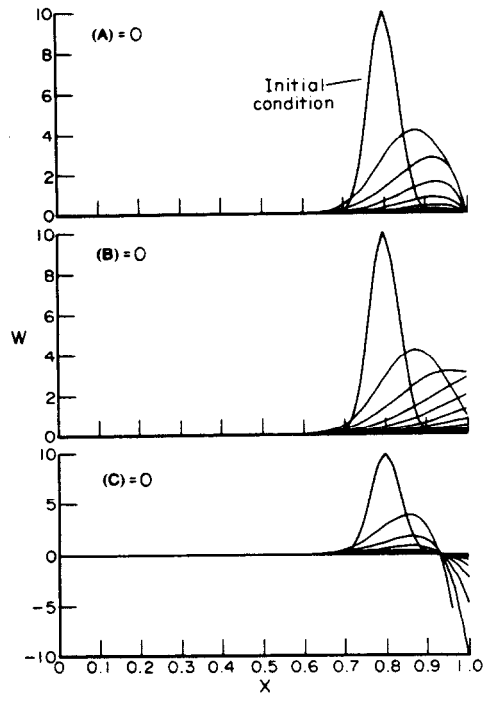

Fig. 5.

Fig. 4. w vs x for incorrect steady state outflow conditions. ($R = 25, J = 50, \Delta t = 0.0025$; plotted every $30\Delta t$).

Fig. 5. w vs x for correct steady state outflow conditions. ($R = 25, J = 50, \Delta t = 0.0025$; plotted every $30\Delta t$).

therefore it seems that this behavior is unaffected by the nonlinearities of the differential equation or by complications of the inflow and initial conditions.

We now turn to the analysis of the continuous equation (2.1) and of its discrete approximation (2.6). Table 1 lists the exact steady state solution of (2.1) with $w_{in} = 0$ and outflow conditions given by (2.12). Also shown is the behavior of w for different values of $\epsilon = 1 - x$ and R. Note that away from $x = 1$, all solutions decay exponentially. Since the solution of the steady state problem without the artificial outflow boundary is identically zero, we see that introducing the artificial boundary causes an error only near $x = 1$. In fact, using our definition of boundary layer thickness we see that $\delta \approx -\ln \sigma / R$ where σ is the "given small percentage." This verifies the experimental result (2.11).

Referring to Table 1, Option B seems to have the advantage of the factor $1/R^2$ in the erroneous boundary layer solution. However, experience shows that errors in the second derivative specification, i.e. B, can often be large, especially when finite disturbances are advecting out of the region at the outflow. Therefore, the advantage of the $1/R^2$ factor may be lost due to the largeness of B. On the other hand Option C seems to have the disadvantage of having a solution proportional to R in the boundary layer. However, due to the exponential decay factor, this does not appreciably affect the solution outside the boundary layer. In fact, at larger Reynolds' number, this "large" solution may help identify the boundary layer.

Table 2 lists the exact steady state solution of (2.6) and the asymptotic rates of convergence

Table 1. Solution of the steady state equation $w_x = w_{xx}/R$ with $w(0) = 0$

Option	Exact solution $w(\epsilon) = w(1-x) =$	Behavior for $\epsilon R \to 0$	Behavior for $\epsilon R = 0(1)$	Behavior for $\epsilon = 0(1)$
$w(1) = A$	$\dfrac{A[e^{-R\epsilon} - e^{-R}]}{1 - e^{-R}}$	$A(1 - \epsilon R)$	$A\, e^{-R\epsilon}$	$0(A\, e^{-R})$
$w_{xx}(1) = B$	$\dfrac{B[e^{-R\epsilon} - e^{-R}]}{R^2}$	$\dfrac{B}{R^2}(1 - \epsilon R)$	$\dfrac{B}{R^2} e^{-R\epsilon}$	$0\left(\dfrac{B}{R^2} e^{-R}\right)$
$\int_0^1 w(x)\, dx = C$	$\dfrac{CR[e^{-R\epsilon} - e^{-R}]}{1 - (1+R)e^{-R}}$	$CR(1 - \epsilon R)$	$CR\, e^{-R\epsilon}$	$0(CR\, e^{-R})$

Table 2. Solution of steady state difference equations. $R_c = Rh/2$, $\lambda = (1+R_c)/(1-R_c)$, J = number of intervals

Option	Exact solution of difference equations $w_i =$	Asymptotic error as $R_c \to 0$ $w_i - w(x_i) =$
A	$\dfrac{A(\lambda^i - 1)}{(\lambda^J - 1)}$	$0(R_c^2)$
B	$\dfrac{Bh^2(\lambda^i - 1)}{(\lambda^J - 2\lambda^{J-1} + \lambda^{J-2})}$	$0(R_c)$
C	$\dfrac{C(\lambda^i - 1)}{h\left\{\dfrac{\lambda^J}{2} + \dfrac{\lambda - \lambda^J}{1-\lambda} - J + \dfrac{1}{2}\right\}}$	$0(R_c^2)$

(as $R_c = Rh/2 \to 0$) to the continuous solution. Note that all three options yield discrete solutions which converge to the corresponding continuous solution. Therefore as $R_c \to 0$, the discrete solutions exhibit the same boundary layer behavior as the continuous solutions. Option B has a slower rate of convergence because of the one sided difference used in (2.9).

Although the above results are for the steady state, a simple perturbation analysis of the unsteady equations show that similar results also hold for the transient solution. Furthermore, we emphasize that the appearance of the boundary layer phenomena near the outflow is in no way tied to the particular choice of discrete approximation used above, e.g. (2.6). This approximation was chosen solely for its simplicity.

3. A 2-D EXAMPLE FOR THE NAVIER-STOKES EQUATIONS

In this section we present computational results for the vorticity and streamfunction in the channel depicted in Fig. 1. Three options for the outflow conditions are considered. Options B and C are analogous to those in Section 2, while for the sake of variety, Option A of that section is replaced by Option A', a specification of first derivatives. Equations (1.1) and (1.2) are discretized by the use of the simple explicit finite difference scheme in which time derivatives are approximated by a forward difference quotient, i.e.

$$\partial\zeta(t_n, x_i, y_j)/\partial t \approx (\zeta_{i,j}^{n+1} - \zeta_{i,j}^n)/\tau$$

and space derivatives are approximated by centered difference quotients, e.g.,

$$\partial^2\psi(t_n, x_i, y_j)/\partial y^2 \approx (\psi_{i,j+1}^n - 2\psi_{i,j}^n + \psi_{i,j-1}^n)/k^2$$

and

$$\partial\zeta(t_n, x_i, y_j)/\partial x \approx (\zeta_{i+1,j}^n - \zeta_{i-1,j}^n)/2h$$

where

$$\zeta_{i,j}^n \approx \zeta(t_n, x_i, y_j), \quad \psi_{i,j}^n \approx \psi(t_n, x_i, y_j)$$

and τ, h and k are the step sizes in t, x and y, respectively. At the inflow boundary (AG in Fig. 1) the flow is assumed to be a fully developed Poiseuille flow so that[8]

$$\psi_{\text{in}} = 4Ud(y/d)^2(1/2 - y/3d) \quad \text{and} \quad \zeta_{\text{in}} = (4U/d)(1 - 2y/d) \tag{3.1}$$

where d is the distance AG and U is the maximum velocity of the Poisseuille profile. Consistent with (3.1), along the upper and lower walls the streamfunction is given by

$$\psi_{\text{low}} = 0 \quad \text{and} \quad \psi_{\text{up}} = 2Ud/3$$

respectively. The wall vorticities are calculated using the Thom formula[2], e.g. along the wall AC

$$\zeta_{i,j}^n = 2(\psi_{i,j}^n - \psi_{i,j-1}^n)/h^2.$$

The initial conditions are $\zeta(t=0)=\psi(t=0)=0$ and our aim is to compute the steady state solutions for ζ and ψ. The fixed parameters used in computing the results discussed below are $R=20$, $h=k=1/16$, $\tau=1/400$, $d=1/2$, the distance $GE=1/2$, and the distance $CD=1$.

In order to complete the specification of the problem we must fix the position of the outflow CD, i. e. choose the distance ED, and then specify outflow conditions on both ζ and ψ. For two of these we choose the specification of the first derivative

$$A': \quad h(\partial\psi/\partial x)|_{CD}=\psi^n_{I,j}-\psi^n_{I-1,j} \tag{3.2}$$

the specification of the second derivative

$$B: \quad h^2(\partial^2\psi/\partial x^2)|_{CD}=\psi^n_{I,j}-2\psi^n_{I-1,j}+\psi^n_{I-2,j} \tag{3.3}$$

and likewise for ζ, where I is the index corresponding to the line CD. For Option C we could approximate the integral

$$I_\psi(t,y)=\int_{-d}^{y}\mathrm{d}y\int_{x_L}^{x_R}\mathrm{d}x\psi(t,x,y)$$

and similarly for I_ζ, where x_R and x_L are respectively the coordinates of the line CD and of the some vertical line to the left of CD. However, approximating these integrals would destroy the compact nature of the approximating scheme since, for instance, any point on the line CD would be coupled to all the points whose y coordinate is smaller. This coupling can be alleviated in two ways, and we use one on I_ψ and the other on I_ζ. Therefore, we impose the outflow conditions

$$I'_\psi=\partial I_\psi/\partial y \quad \text{and} \quad \Delta I_\zeta=I_\zeta(t,y)-I_\zeta(t,y-k) \tag{3.4}$$

which can be approximated by

$$C: \quad I'_\psi(n\tau,jk)=\frac{h}{2}\left(\psi^n_{I-p,j}+2\sum_{i=I-p+1}^{I-1}\psi^n_{i,j}+\psi^n_{I,j}\right) \tag{3.5a}$$

and

$$\Delta I_\zeta(n\tau,jk)=\frac{hk}{4}\sum_{i=I-p+1}^{I}(\zeta^n_{i,j}+\zeta^n_{i-1,j}+\zeta^n_{i-1,j-1}+\zeta^n_{i,j-1}) \tag{3.5b}$$

where x_L and x_R are chosen so that $x_R-x_L=ph$. The choice for I'_ψ is particularly important because it preserves the bandwidth of the matrix appearing in the discrete approximation to (1.2).

We first choose to place the outflow boundary CD "far" downstream, e.g. $ED=4d=2$, and we then assume that at this position the flow has settled into a fully developed Poiseuille flow in a channel of width $2d$. Then the left hand sides of (3.2), (3.3) and (3.5) may be computed analytically by using (3.1) with (y/d) replaced by $(y+d)/2d$. Computational results show that the solutions due to the three options for the outflow condition are identical in the sense that their pointwise differences (suitably scaled by average values of the variables) are uniformly less than 10^{-4}, which is considerably less than the discretization error of the finite difference scheme. These results are not surprising since we have imposed accurate outflow conditions on both ψ and ζ. This calculation was performed in order to provide a benchmark for the computations reported below.

We now move the outflow boundary CD "close" to the corner point F by choosing $ED=d=1/2$ (or $x_{CD}=1$). We use the results of the above "exact" calculation to evaluate the left hand sides of the outflow conditions (3.2), (3.3) and (3.5). The computational results for all three options are again indistinguishable from each other and from the above "exact" calculation. This shows that for any type outflow condition, including integral conditions, a correct specification will yield correct solutions even when the outflow is in a region of significant flow changes.

With the outflow still at $x = 1$, we next purposely choose incorrect outflow conditions for both ψ and ζ by choosing the left hand side of all outflow conditions to be zero. The results were poor for all three options. Typical pointwise differences (again suitably scaled) between these calculations and the "exact" ones described above were of the order of 10^{-1} to 10^{-2}. These results, denoted below as being "incorrect," indicate that if the outflow conditions are incorrectly specified, then the solution will be adversely affected everywhere.

We now examine the effect of imposing correct outflow conditions on ψ and incorrect ones on ζ. This is of interest because it is in general much easier to obtain information on ψ, which depends on integrals of the velocity, than on ζ, which depends on derivatives of the velocity. We label this calculation "correct–incorrect". In Fig. 6 we show $(\psi_I - \psi_E)/\bar{\psi}_E$ and $(\psi_{CI} - \psi_E)/\bar{\psi}_E$ along the line FB of Fig. 1 and in Fig. 7 we show $(\zeta_I - \zeta_E)/\bar{\zeta}_E$ and $(\zeta_{CI} - \zeta_E)/\bar{\zeta}_E$ along the line HK of Fig. 1 where the subscripts I, CI and E refer to the "incorrect," "correct–incorrect" and "exact" calculations respectively, and the bar indicates the average value of the variable. These results are typical of those throughout the flow field. From both figures we see that by imposing correct outflow conditions on ψ, we can significally improve the solution. The errors of the "correct–incorrect" run are, except near the outflow, typically smaller than $h^2 = 1/256$ which is a

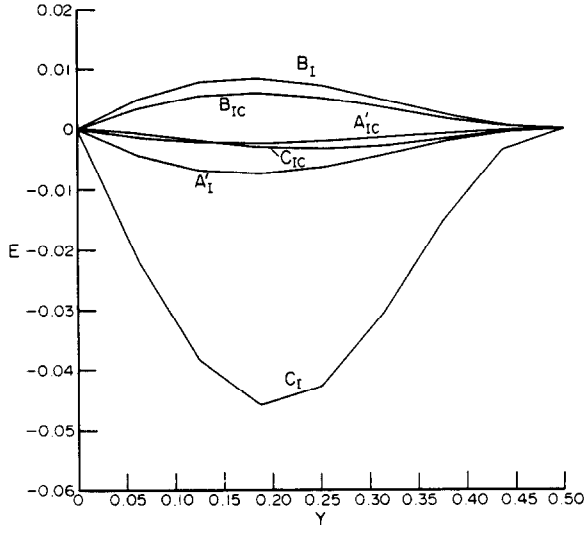

Fig. 6. Error in the steady state streamfunction at $x = 1/2$. $[E = (\Psi - \Psi_E)/\bar{\Psi}_E]$ ($R = 20$, $\Delta x = \Delta y = h = 1/16$; I = "incorrect" calculation, IC = "incorrect–correct" calculation).

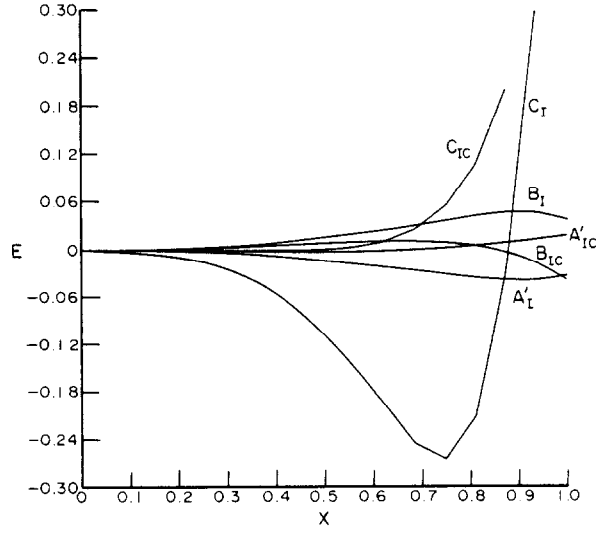

Fig. 7. Error in the steady state vorticity at $y = 1/4$. $[E = (\zeta - \zeta_E)/\bar{\zeta}_E]$ ($R = 20$, $\Delta x = \Delta y = h = 1/16$; I = "incorrect" calculation, IC = "incorrect–correct" calculation).

liberal estimate for the discretization error. For the "incorrect" run, the errors are considerably larger than h^2. In Fig. 7, the boundary layer phenomena described in Section 2 is not as sharply evident because both the ellipticity of the Poisson equation and the nonlinearity of the equations contribute to the smearing of the boundary layer. However, experiments at different Reynolds' numbers confirm that the boundary layer thickness decreases with increasing Reynolds' number. Also note that for the "correct–incorrect" run that Option C has a large error in the boundary layer, but in the interior it is of the same magnitude as the other options. This type of behavior is similar to that encountered in Section 2.

There is no reason why one should use the same type of outflow conditions for the ψ and ζ. One could mix the options, choosing judiciously according to the information available, or in the absence of complete information, experimenting to determine which combination least affects the solution of the specific problem considered.

To summarize, the computational results of this section indicate that an incorrect specification of outflow conditions will result in spurious solutions away from the outflow boundary while a correct specification will result in a correct solution everywhere regardless of which option for the outflow condition is chosen. Furthermore, the results of Section 2 extend to two dimensions and to the full Navier–Stokes equations in the sense that if we correctly specify ψ at the outflow, but incorrectly specify ζ, then the errors in the solution are small for large portions of the computational domain and are large only in the vicinity of the outflow boundary. Finally, we have seen that integral outflow conditions on both ζ and ψ are not only implementable, but affect the solution of (1.1) and (1.2) in much the same manner as commonly used outflow conditions.

4. ANALYSIS OF INTEGRAL CONDITIONS FOR THE POISSON EQUATION

For arbitrary two dimensional domains an attempt to prove that the Poisson equation (1.2) with an integral condition such as (3.4) imposed on part of the boundary (and Dirichlet data on the rest) constitute a well posed problem would lead us to a complicated analysis involving integral equations. To avoid these complications we consider the model problem

$$\nabla^2 u = f \quad \text{in} \quad \Omega = [0, 1] \times [0, 1] \tag{4.1}$$

$$u = 0 \quad \text{on} \quad \Gamma_1 \tag{4.2}$$

and

$$\int_0^y dy' \int_\alpha^1 dx u(x, y') = \gamma(y) \quad \text{on} \quad \Gamma_2 = \{(1, y) | 0 \le y \le 1\} \tag{4.3}$$

where α is a fixed number, $0 < \alpha < 1$, and where $\Gamma_1 \cup \Gamma_2 = \Gamma$, the boundary of the region Ω. Figure 8 shows the regions Ω and Ω_Y, the latter being the domain of integration of the integral appearing in (4.3). The central idea in our analysis is to solve the Dirichlet problem defined by (4.1), (4.2) and

$$u = \theta(y) \quad \text{on} \quad \Gamma_2, \tag{4.4}$$

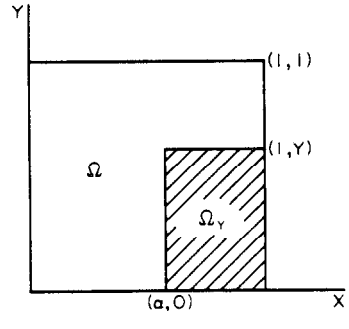

Fig. 8. The regions Ω and Ω_Y.

and to choose θ so that (4.3) is satisfied. To do this we observe that the solution of (4.1), (4.2) and (4.4) is

$$u(x, y) = U(x, y|f) + \int_{\Gamma_2} g(x, y|\eta)\theta(\eta)\,d\eta$$

where

$$U(x, y|f) = \int_\Omega \int G(x, y, \xi, \eta) f(\xi, \eta)\,d\xi\,d\eta,$$

$G(\cdot, \cdot, \cdot, \cdot)$ is the Green's function for the homogeneous problem ((4.1) plus $u = 0$ on Γ) and g is the normal derivative of G restricted to Γ_2.

We conclude that (4.1), (4.2) and (4.3) have a (unique) solution if and only if

$$\gamma_1(y) = \int_{\Gamma_2} \hat{g}(y, \eta)\theta(\eta)\,d\eta, \quad 0 \le y \le 1 \tag{4.5}$$

has a (unique) solution. In (4.5)

$$\gamma_1(y) = d\gamma/dy - \int_\alpha^1 dx U(x, y|f)$$

and

$$\hat{g}(y, \eta) = \int_\alpha^1 dx g(x, y|\eta).$$

Simple calculations verify that

$$\int_{\Gamma_2} g(x, y|\eta)\theta(\eta)\,d\eta = \sum_{k=1}^{\infty} \theta_k \frac{\sinh(k\eta x)}{\sinh(k\pi)} \sin(k\pi y)$$

where

$$\theta(y) = \sum_{k=1}^{\infty} \theta_k \sin(k\pi y).$$

Thus our integral equation (4.5) becomes

$$\gamma_1(y) = \sum_{k=1}^{\infty} \theta_k \left\{ \frac{\cosh(k\pi) - \cosh(k\pi\alpha)}{k\pi \sinh(k\pi)} \right\} \sin(k\pi y)$$

and thus the unique solvability of (4.5) is clear.

This calculation also shows that the mean square norm of second derivatives of u is bounded above by the mean square norm of f plus the "5/2 norm" of γ, i.e.

$$\|\gamma\|_{5/2} = \left\{ \sum_{k=1}^{\infty} k^5 \gamma_k^2 \right\}^{1/2} \tag{4.6}$$

where

$$\gamma(y) = \sum_{k=1}^{\infty} \gamma_k \sin(k\pi y).$$

This shows that the problem is well posed in the sense that small changes in γ with respect to (4.6) leads to small changes in u, ∇u and the second derivatives of u in the mean square sense.

Turning to approximations let us consider a uniform grid with nodes at (ih, jh), $0 \le i, j \le N = 1/h$. We approximate $u(ih, jh)$ with $u_{i,j}$ where

$$[4u_{i,j} - u_{i,j+1} - u_{i,j-1} - u_{i+1,j} - u_{i-1,j}] + h^2 f(ih, jh) = 0 \tag{4.7}$$

for $0 < i, j < 1/h$, and with

$$u_{i,j} = 0 \quad \text{for} \quad \begin{cases} i = 0, & 0 \le j \le 1/h \\ 0 \le i \le 1/h, & j = 0 \\ 0 \le i \le 1/h, & j = 1/h \end{cases} \tag{4.8}$$

At the nodes for which $x = 1$, $0 < y < 1$, we use

$$\frac{h}{2} \sum_{i=i_0}^{(1/h)-1} [u_{i+1,j} + u_{i,j}] = \frac{d\gamma}{dy}(jh) = \gamma_1(jh) \tag{4.9}$$

for $0 < j < 1/h$. We assume that $\alpha = (i_0 h)$ and without loss of generality we take $f = 0$. The exact solution is thus

$$u(x, y) = \sum_{k=0}^{\infty} \theta_k \frac{\sinh(k\pi x)}{\sinh(k\pi)} \sin(k\pi y). \tag{4.10}$$

A straightforward calculation shows that the solution of (4.7), (4.8) and

$$u_{N,j} = \theta(jh) = \sum_{k=0}^{1/h} \theta_k^h \sin(k\pi jh), \quad 0 < j < 1/h$$

is given by

$$u_{i,j} = \sum_{k=0}^{1/h} \theta_k^h \left\{ \frac{\sinh(k\pi ih)}{\sinh(k\pi)} \right\} \sin(k\pi jh) + 0(h^2). \tag{4.11}$$

With this representation the unique solvability of (4.9) is clear once we note that

$$\frac{h}{2} \sum_{i=i_0}^{(1/h)-1} \{\sinh[k\pi ih] + \sinh[k\pi(i+1)h]\} \to \frac{\cosh(k\pi) - \cosh(k\alpha\pi)}{k\pi}$$

as $h \to 0$. To be sure the difference between the trapezoidal rule quadrature on the left and the exact quadrature on the right is $0(h^2)$, and with this it is easy to see that θ_k^h in (4.11) differs from θ_k in (4.10) by $0(h^2)$. An additional calculation gives

$$u(ih, jh) - u_{i,j} = 0(h^2) \quad \text{as} \quad h \to 0.$$

Therefore the integral boundary condition (4.3) and its discrete implementation (4.9) do not adversely affect the accuracy of the finite difference scheme.

Acknowledgement—This paper was prepared as a result of work performed under NASA Contract No. NAS1-14101 while the authors were in residence at ICASE, NASA Langley Research Center, Hampton, VA 23665, U.S.A.

REFERENCES

1. S. I. Cheng, Numerical intergration of Navier–Stokes equations, *A.I.A.A. Jl*, **8** 2115–2122 (1970).
2. P. Roache, *Computational Fluid Dynamics*. Hermosa, Albuquerque (1972).
3. J. Paris and S. Whitaker, *A.I.Ch.E. Jl.* **11** 1033 (1965).
4. R. L. Cerro and S. Whitaker, *Chem. Engng Sci.* **26**, 785 (1971).
5. R. L. Cerro and S. Whitaker, *Comput. Fluids* **3**, 321 (1974).
6. K. N. Ghia, AIAA Paper No. 74-559, June 1974.
7. *Dynamics and the Analysis of Mode* 1, Report of the Mode One Group. MIT Publications, Cambridge (1975).
8. H. Schlichting, *Boundary Layer Theory*. McGraw-Hill, New York (1951).